Updated Mean Sea-Level Analysis: South Korea

Updated Mean Sea-Level Analysis: South Korea

Phil J. Watson

Coastal Education and Research Foundation (CERF)
Coconut Creek, FL 33073, U.S.A.
philwatson.slr@gmail.com

www.cerf-jcr.org

www.JCRonline.org

ABSTRACT

Watson, P.J., 2019. Updated mean sea-level analysis: South Korea. *Journal of Coastal Research,* 35(2), 241–250. Coconut Creek (Florida), ISSN 0749-0208.

The threat of sea-level rise to the heavily populated Korean Peninsula has profound and far-reaching implications. This study updates and extends the several previous works undertaken to analyse tide-gauge records and satellite altimetry around South Korea using enhanced time-series analysis techniques to detect coastal vertical land motion and current rates of rise and accelerations in mean sea level to augment planning, design, and risk management activities. Although the longest tide-gauge records available only date back to 1960, every effort has been made to separate the mean sea-level trend from the more dynamic influences with improved precision using state-of-the-art analytical techniques. The analysis identified general trends of subsidence observed around the margins bounded by the East China Sea and East Sea (Sea of Japan) below 36°N, whereas uplift was a more prevalent feature along the margins bounded by the Yellow Sea. All tide-gauge records longer than 50 years exhibited 'relative' mean sea-level rise increasing marginally over the length of the record, suggesting the presence of an acceleration; however, the estimated time-varying accelerations (albeit predominantly positive) are small and not statistically different from zero (95% confidence interval). Although the average trend of sea-surface height from satellite altimetry across this region was 3.2 mm/y, key spatial variations were evident, with the highest rates of rise centred in two discrete areas east and west of South Korea around 37.5°N, each exceeding 8 mm/y.

ADDITIONAL INDEX WORDS: *Sea-level rise, climate change, velocity, acceleration, vertical land motion.*

INTRODUCTION

A rising global mean sea level provides increasing risks to coastal communities associated with saltwater inundation and flooding. These risks are heightened by ever-increasing populations occupying the low-elevation coastal zone ($<$10 m above mean sea level) around the globe (McGranahan, Balk, and Anderson, 2007), fuelled by a trend of coastal population migration (Neumann *et al.*, 2015). Flood exposure is increasing in coastal cities owing to growing populations and assets, the changing climate, and land subsidence (Hallegatte *et al.*, 2013).

A recent economic analysis of the cost of climate-change impacts around the Korean Peninsula (Yeora, 2012) estimated the economic damage arising from coastal erosion and flood damage associated with sea-level rise to 2100 (on the basis of the Intergovernmental Panel on Climate Change A1B scenario) to be of the order of 7.5 trillion won (USD 6.7 billion). Scientific projections (Church *et al.*, 2013) forecast mean sea level continuing to rise at increasing rates over the course of the 21st century (and beyond) as a result of climate change. Such forecasts place renewed efforts on adaptation and mitigation planning to reduce risk to an acceptable or manageable level.

The prominence of the climate change issue has placed more emphasis on examination of the extensive global repository of relative mean sea-level records (Holgate *et al.*, 2012), which, along with temperature and carbon dioxide, remain the key proxy data sets used to monitor and quantify changes in the global climate system (Watson, 2016a). Mean sea-level records measured at coastal tide gauges provide the optimum means of detecting changes in the rate of sea-level rise over time, particularly when the length of the records extends beyond 80–100 years. However, it's imperative to understand that the water level measured at a tide gauge is a complex amalgam of key physical contributors which include (1) vertical land movement at the tide-gauge site (factor 1); (2) dynamic influences of largely oceanographic, atmospheric, or gravitational origins operating on differing temporal and spatial scales (factor 2); and (3) low-amplitude signal of mean sea-level rise driven by climate-change influences (principally melting of snow and ice reserves bounded above sea level [directly adding water], and thermal expansion of the ocean water mass) (factor 3).

This study updates and extends the previous works undertaken to analyse tide-gauge records and satellite altimetry around the Korean Peninsula (*e.g.*, Ha *et al.*, 2006; Jeon, 2008; Kang *et al.*, 2005; KHOA, 2013; Kim and Cho, 2016; Kim *et al.*, 2017; Yoon, 2016). In particular, the longer tide-gauge records available ($>$50 y) have been analysed using enhanced time-series analysis techniques developed specifically for mean sea-level research (Watson, 2018) that improve the resolution of the factor 3 influence. The study also provides updated, consistent estimates of the factor 1 influence based on analysis of gridded satellite altimetry data for the Korean region, providing improved instruction on areas likely to be more susceptible to "relative" mean sea-level rise resulting from vertical land motion (VLM).

Data Sources Used in this Study

Annual and monthly average time-series data from the public archives of the Permanent Service for Mean Sea Level (PSMSL) (Holgate *et al.*, 2012; PSMSL, 2018) have
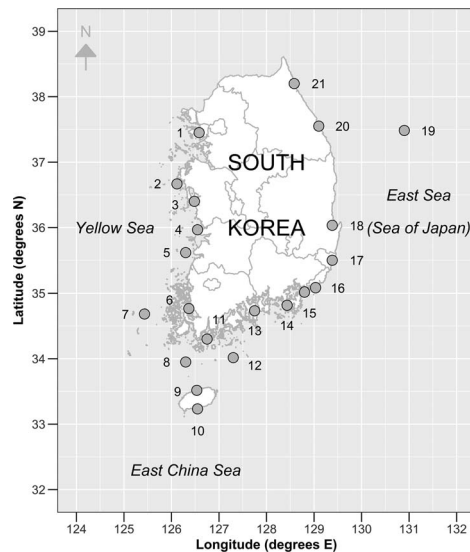
Figure 1. Location of tide-gauge records analysed for this study. Sites have been delineated with a station ID commencing with 1 (Incheon) and moving anticlockwise to 21 (Sokcho). Full details of data records are summarized in Table 1. Base plan generated using ggmap package (Kahle and Wickham, 2013) in R (R Core Team, 2018).

been used in the analysis, up to and including 2017. The 21 sites analysed have notionally been assigned a station identification (ID) commencing with Incheon (1) in the NW, progressing anticlockwise around the country to Sokcho in the NE, bordering the East Sea (Sea of Japan) (refer Figure 1).

Satellite altimeter products by Ssalto/Duacs distributed by Archiving, Validation and Interpretation of Satellite Oceanographic (AVISO), with support from the Centre National d'Etudes Spatiales (CNES) (AVISO, 2018), have been used to extract time series of sea-surface heights. These data have been made available for this research in netCDF format from the Integrated Climate Data Center (ICDC) (ICDC, 2018), with daily outputs spanning the period 1 January 1993 to 15 May 2017 on a spatial resolution grid of $0.25° \times 0.25°$ (Cartesian). Daily outputs have been converted into monthly average time series at the nearest grid point to the respective tide-gauge record (refer to Table 1 for details) and compared with the monthly average tide-gauge record to estimate VLM at each station.

METHODS

Differing methodologies have been applied in this study, dependent upon the specific analysis and the length of the respective data sets. The applied methodology can be appropriately partitioned into analysis of the historical tide-gauge records, sea-surface heights from satellite altimetry, and estimates of VLM. All analysis and graphical outputs have been developed by the author from customized scripting code within the framework of the R Project for Statistical Computing (R Core Team, 2018).

Historical Tide-Gauge Analysis

The complexity of the influences embedded within conventional monthly and annual average ocean water-level data sets has led sea-level research toward successively more sophisticated time-series analytical techniques. The key prerogative for sea-level researchers remains isolating the comparatively small, nonstationary, nonlinear mean sea-level signal from the significant and substantial dynamic interdecadal (and other)

Table 1. Summary of data used in this study.

Station ID[‡]	Location	Tide-gauge data East	North	Start (y)	End (y)	Length (y)	Nearest AVISO grid[†] East	North	Distance to tide gauge (km)
1	Incheon	126°34′58.7994″	37°27′	1960	2017	57	126°37′30″	37°22′30″	9.11
2	Anheung	126°7′1.2″	36°40′1.2″	1989	2017	28	126°7′30″	36°37′30″	4.68
3	Boryeong	126°28′58.8″	36°23′59.9994″	1986	2017	31	126°22′30″	36°22′30″	10.10
4	Gunsan	126°32′59.9994″	35°58′1.1994″	1981	2017	36	126°37′30″	35°52′30″	12.22
5	Wido	126°17′59.9994″	35°37′1.1994″	1985	2017	32	126°22′30″	35°37′30″	6.86
6	Mokpo	126°22′1.2″	34°46′1.2″	1960	2017	57	126°22′30″	34°52′30″	12.04
7	Heuksando	125°25′58.8″	34°40′58.7994″	1979	2017	38	125°22′30″	34°37′30″	8.39
8	Chujado	126°17′59.9994″	33°37′	1984	2017	33	126°22′30″	33°52′30″	10.83
9	Jeju	126°31′58.8″	33°31′1.2″	1964	2017	53	126°37′30″	33°37′30″	14.72
10	Seogwipo	126°32′59.9994″	33°13′58.7994″	1985	2017	32	126°37′30″	33°7′30″	13.90
11	Wando	126°45′	34°17′59.9994″	1983	2017	34	126°37′30″	34°22′30″	14.20
12	Geomundo	127°17′59.9994″	34°1′1.2″	1982	2017	35	127°22′30″	34°7′30″	13.87
13	Yeosu	127°45′	34°43′58.7994″	1966	2017	51	127°37′30″	34°37′30″	16.60
14	Tongyeong	128°25′58.7994″	34°49′1.2″	1977	2017	40	128°22′30″	34°52′30″	8.38
15	Gadeokdo	128°48′	35°1′1.2″	1977	2017	40	128°52′30″	35°7′30″	13.84
16	Busan	129°1′58.7994″	35°4′58.7994″	1960	2017	57	129°7′30″	35°7′30″	9.56
17	Ulsan	129°22′58.8″	35°30′	1962	2017	53	129°22′30″	35°22′30″	13.89
18	Pohang	129°22′58.8″	36°1′58.8″	1972	2016	34	129°22′30″	36°7′30″	10.20
19	Ulleung	130°54′	37°28′58.7994″	1979	2017	38	130°52′30″	37°22′30″	12.22
20	Mukho	129°5′59.9994″	37°32′59.9994″	1965	2017	52	129°7′30″	37°37′30″	8.61
21	Sokcho	128°34′58.7994″	38°12′	1974	2017	43	128°37′30″	38°7′30″	9.09

[†]Nearest satellite altimetry grid point to tide-gauge record with data coverage.
[‡]Station ID is a local referencing protocol used throughout this study. Refer to Figure 1 for plan location.

influences and noise. This is achieved through the application of singular spectrum analysis (SSA) techniques adapted specifically for mean sea-level research (Watson, 2018).

SSA has proven an optimal analytic for this task in sea-level studies (Watson, 2016b) as a powerful data-adaptive technique capable of decomposing a time series into the sum of interpretable components with no *a priori* information about the time-series structure (Alexandrov *et al.*, 2012; Golyandina and Zhigljavsky, 2013). Specifically, SSA can efficiently decompose an original record into a series of components of slowly varying trend, oscillatory components with variable amplitude, and a structureless noise (Golyandina, Nekrutkin, and Zhigljavsky, 2001).

Only the longest annual average records available from the PSMSL (>50 y) were considered for trend analysis (refer to Discussion on length of records). The methodology applied in analysing the observational tide-gauge records can be broadly summarised in the following five steps.

Step 1: Gap-Filling of Time Series

This is a necessity to decompose the time series using SSA. Although the longest and most complete tide-gauge records have been used for analysis, missing data persist in several records. Where required, records have been filled using an iterative SSA procedure (Kondrashov and Ghil, 2006) in the first instance, which has an (assumed) advantage in preserving the principal spectral structures of the complete portions of the original data set in filling the gaps.

Step 2: Estimation of Relative Mean Sea Level

Having necessarily filled the time series in step 1, the record is decomposed using one-dimensional SSA to isolate components of slowly varying trend (*i.e.* mean sea level due to external climate forcing) from oscillatory components with variable amplitude, and noise. From the SSA decomposition, relative mean sea level is estimated by summation of "trend-like" components. To do this, a periodogram is fitted to each of the decomposed components with trend-like components specifically determined to be those in which the peak spectral density is confined to the lowest-frequency band.

Step 3: Estimation of Relative Mean Sea-Level Velocity and Acceleration

Readily estimated from the first and second derivatives, respectively, of a cubic smoothing spline fitted to the mean sea level (or trend) determined via step 2. In each case, a fitted spline with 1 degree of freedom every 10 years results in the coefficient of determination (R^2) of the fitted spline to the sea-level trend exceeding 0.99, providing a high degree of confidence in this form of model to estimate the associated time-varying velocity and acceleration.

Step 4: Estimation of Errors

This process initially involves fitting an autoregressive time-series model to remove the serial correlation in the residuals between the SSA-derived trend (step 2) and the gap-filled time series (step 1). The estimation of error in the relative mean sea level and associated velocities is then based on bootstrapping techniques where the uncorrelated residuals are randomly recycled and the process in steps 2 and 3 repeated 1000 times. From the extensive pool of outputted relative mean sea level and associated velocities and accelerations, standard deviations are readily calculated to derive robust confidence intervals.

Step 5: Correction to Estimate Geocentric Velocity

The correction from relative to geocentric velocity has been undertaken using the approach of Ostanciaux *et al.* (2012) (refer section 3.2). Error margins in quantifying geocentric velocity are determined in quadrature.

VLM Analysis

Following the approach advocated by Ostanciaux *et al.* (2012), VLM is estimated by applying a least-squares linear regression fit to the difference between the monthly averages derived from satellite altimetry and the relative tide-gauge record at a point of interest. More specifically, to estimate VLM at a specific tide-gauge site, the methodology applied can be broadly summarised in the following three steps.

Step 1: Determine Nearest AVISO Grid Reference with Data

The available AVISO satellite altimetry data are provided on a spatial resolution grid of $0.25° \times 0.25°$; thus the initial step is to isolate the nearest grid reference point to the tide-gauge location that contains complete sea-surface height data (summarised in Table 1).

Step 2: Convert Daily AVISO Sea-Surface Height Time Series to Monthly Averages

Complete monthly average time series of sea-surface heights are available spanning the period from January 1997 to April 2017.

Step 3: Linear Regression Analysis

VLM can be estimated from linear regression of the difference between the respective monthly average of the AVISO altimetry (step 2) and the tide-gauge time series spanning January 1997 to April 2017. VLM is estimated as a rate (mm/y) with associated standard errors. The estimated VLM can then be used to correct relative to geocentric velocity at each of the tide-gauge sites.

Altimetry Sea-Surface Height Analysis

Daily AVISO sea-surface height time series have been extracted at each of the respective grid points covering an area around South Korea extending from 124 to 132°E and 32 to 39°N to investigate spatial trends evident over the altimetry data period. The trend in sea-surface height has been determined at each grid reference point on the basis of simple linear regression techniques.

RESULTS

Of importance, all analysis results presented in this report include error margins at the 95% confidence level, unless noted otherwise. Analysis of the seven tide-gauge records exceeding 50 years provides the means to optimise estimates in the temporal resolution of relative mean sea level and associated velocity and acceleration over time. It is evident from the analysis of each of these records (refer Figure 2) that the relative velocity has varied over time, but continued to rise at each site over the course of the record, suggesting the presence of an acceleration to do so.
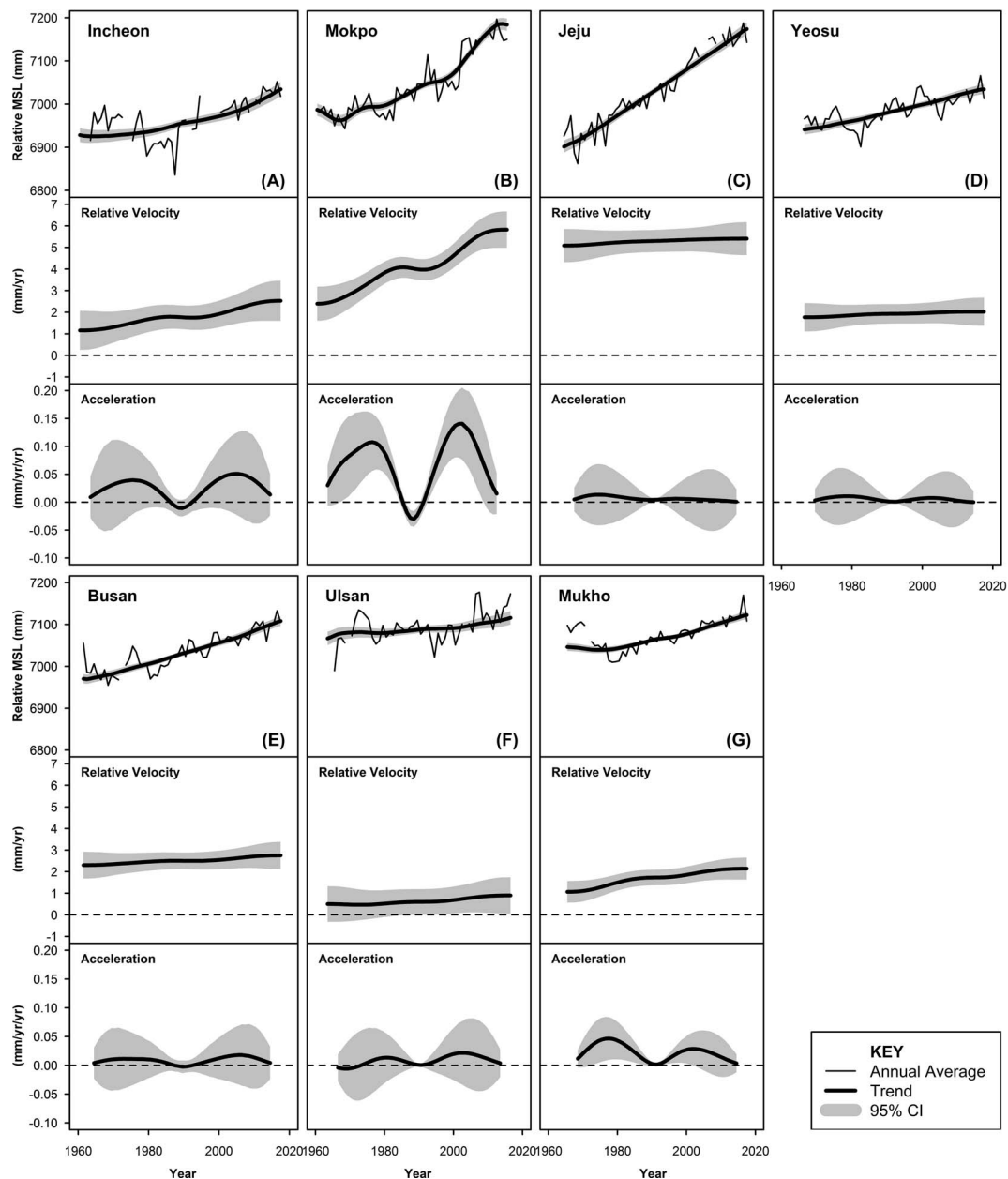
Figure 2. Relative mean sea level (trend) and associated velocity and acceleration from records longer than 50 years. The scales associated with each of the three panel charts for the respective tide-gauge records are equivalent for direct comparison between records. Refer to Figure 1 and Table 1 for station details.

The temporal characteristics of the time-varying relative velocity highlight similarities between each record, with differences in the scale (in part) reflective of the underlying VLM embedded within the respective records (see Figure 3). The highest rates of relative mean sea-level rise were observed at Mokpo and Jeju (5.8 ± 0.8 and 5.4 ± 0.8 mm/y, respectively) over the recent portion of the record. Both sites exhibit subsidence at rates exceeding 3 mm/y. Of the remaining five long record sites, the rate of relative mean sea-level rise observed during 2017 varied between 0.9 ± 0.8 and 2.8 ± 0.6 mm/y (see Figure 3).

The associated time-varying acceleration in mean sea level at each of the data records exceeding 50 years in length highlights key temporal signatures in the coastal margins around South Korea (see Figure 2). For the majority of records analysed, the estimated accelerations (albeit predominantly positive) are small and not statistically different from zero at the 95% confidence level, with exceptions at Mokpo and Mukho. Strong temporal signatures persist across the network of records analysed, with peak accelerations evident in time frames spanning 1974 to 1980 and again around 2002 to 2006, and
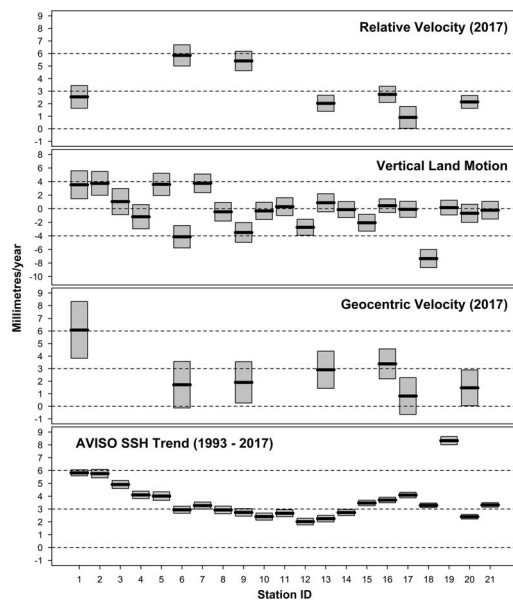
Figure 3. Summary of results. Only station records longer than 50 years have been used to determine relative and geocentric velocities in 2017. All analysis relates to 2017 except for Mokpo (ID = 6), where the annual record ends in 2015. Refer to Figure 1 and Table 1 for station ID details. Shaded boxes represent 95% confidence intervals in each panel. For details on the methodology underpinning the respective charts, refer to Methods.
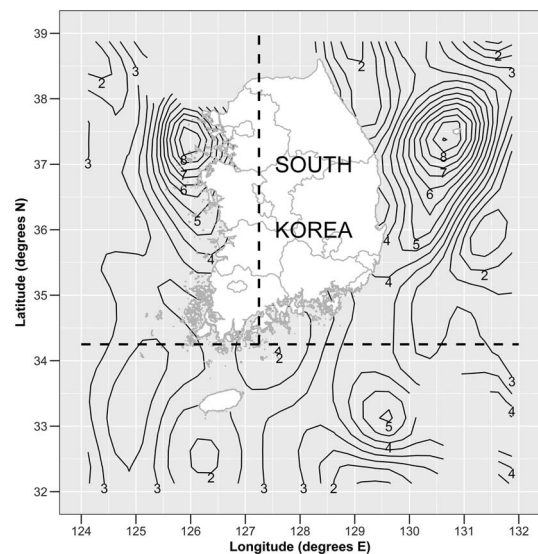

Figure 4. Sea-surface height trends from satellite altimetry (1993–2017). Trends are based on linear regression of the complete time series at each grid point spanning the period 1 January 1993 to 15 May 2017. Black dashed lines arbitrarily demarcate the respective Yellow Sea, East Sea (Sea of Japan), and East China Sea margins around South Korea for analysis purposes only.

minimum accelerations (some negative) observed between 1988 and 1992. The largest acceleration measured was 0.14 $\pm$ 0.06 mm/y^2 at Mokpo in 2002. Acceleration in mean sea level has moderated post-2005 to present at all sites.

From the VLM analysis at the respective tide gauges, general trends of subsidence were observed around the margins bounded by the East China Sea and East Sea (Sea of Japan) (below 36°N), whereas uplift was a more prevalent feature along the margins bounded by the Yellow Sea. The highest rates of uplift were observed at Heuksando and Anheung (3.7 $\pm$ 1.4 and 3.7 $\pm$ 1.7 mm/y, respectively), with Wido and Incheon both exceeding 3.5 mm/y. The highest rates of subsidence were observed at Pohang, Mokpo, and Jeju (−7.4 $\pm$ 1.3, −4.1 $\pm$ 1.6, and −3.5 $\pm$ 1.5 mm/y, respectively). Estimates of VLM at each gauge site are summarised in Figure 3 (second panel).

The third panel of Figure 3 provides a summary of the estimated geocentric velocity in 2017 for each of the records longer than 50 years, following corrections for VLM. Excluding Incheon, geocentric velocities lie broadly in the range of ≈1 to 3 mm/y. Of interest, the geocentric velocity estimated at Incheon in 2017 is considerably higher than all the other stations, at 6.1 $\pm$ 2.2 mm/y. Of the records exceeding 50 years in length, Incheon has the highest percentage of missing data (≈9%), which might have a bearing on both the accuracy of the derived trend of relative mean sea level and also the estimate of VLM derived from the difference between the satellite altimetry record and that of the tide gauge. Notwithstanding, this high rate mirrors the equally high trend in sea-surface height measured from satellite altimetry at Incheon over the period

from 1993 to 2017 (5.82 $\pm$ 0.24 mm/y; see Figure 3 bottom panel).

Trends in sea-surface height observed from AVISO satellite altimetry data over the period from 1993 to 2017 (between 124 and 132°E and 32 and 39°N) show some key spatial signatures (see Figures 3 and 4, Table 2) around South Korea.

Of the 1041 gridded data points, the average trend of sea-surface height across this region was 3.21 $\pm$ 0.29 mm/y. The highest average sea-surface height trends were centred in two discrete areas east and west of South Korea around 37.5°N, each exceeding 8 mm/y (see Figure 4). Within the respective Yellow Sea, East Sea (Sea of Japan), and East China Sea margins analysed, some differences are evident. Although the average trends across each sea margin and the global average (3.62 $\pm$ 0.47 mm/y) are aligned at the 95% confidence level (see Table 2), the means differ and are all below the global average,

Table 2. *Summary of sea-surface height trends from satellite altimetry.*

Area	Average sea-surface height trend (mm/y)[†]	AVISO grid points analysed
Region encompassing South Korea[‡]	3.21 $\pm$ 0.29	1041
Yellow Sea[‡]	3.33 $\pm$ 0.31	361
East Sea (Sea of Japan)[‡]	3.54 $\pm$ 0.27	275
East China Sea[‡]	2.88 $\pm$ 0.31	405
Global mean sea level[§]	3.62 $\pm$ 0.47	—

[†]*95% confidence intervals advised.*
[‡]*Refer to Figure 4 for extent of regional assessment and arbitrary demarcation of the respective sea margins (for analysis purposes only). Analysis spans period from January 1993 to May 2017.*
[§]*Global mean sea-level estimate from AVISO (2018) for the period 1 January 1993 to 4 June 2018, excluding allowances for GIA.*

with the South China Sea average approximately 0.75 mm/y lower over the 24-year record.

Immediately adjacent to the coastline, the sea-surface height trends nearest the respective tide-gauge locations (see Figure 3, bottom panel) show a finer-resolution spatial pattern in which the peak trends (>5 mm/yr) are observed east and west at around 37.5°N, moderating generally in a southerly direction around the country, with the lowest trend adjacent to a tide gauge observed at Geomundo (2.02 ± 0.25 mm/y).

It should be clearly emphasised here that these linear trends in sea-surface height over the 24-year altimetry period will be significantly influenced by internal climate mode forcings (such as El Niño–Southern Oscillation [ENSO], *etc.*) on such timescales. These trends are therefore not directly comparable with relative and geocentric velocities determined from the longer tide-gauge records analysed in this study, which first remove such influences from the record and second, estimate time-varying velocities in real time, rather than averages across the record length.

DISCUSSION

Watson (2018) notes that the length of the data sets available is a key facet to improving the robustness of trend, velocity, and acceleration estimates derived from long, individual ocean water-level records. For example, Douglas (2001) advised minimum-length data sets of 50–60 years to measure acceleration to lower the likelihood of key contamination from the influences of decadal to multidecadal variability that ostensibly result from winds driven by climate modes (see Qiu and Chen, 2012; Sturges and Douglas, 2011). Through further detailed analysis, Houston and Dean (2013) advised that, because of decadal variations, record lengths of at least 75 years should be used to determine acceleration, and even longer records should be used to determine trend differences.

Chambers, Merrifield, and Nerem (2012) identified the existence of a significant oscillation with a period around 60 years in the majority of the tide gauges examined during the 20th century, and that it appears in every ocean basin, with amplitudes exceeding 20 mm in several long records. Chambers, Merrifield, and Nerem (2012) and Calafat and Chambers (2013) advise that estimates of global and regional accelerations must account for these multidecadal fluctuations.

Watson (2018) recommends the use of annual time series of minimum length 80 years to ensure the trend signal (or in this case mean sea level) is optimally separable from the contaminating dynamic cyclical signals (including the quasi-60-year ocean oscillation proposed by Chambers, Merrifield, and Nerem [2012]) and noise.

The maximum-length data sets available for this analysis around the South Korean Peninsula are 57 years (1960 to 2017 at Incheon, Mokpo, and Busan), somewhat short of the optimal minimum lengths suggested for mean sea-level analysis. The results of the analysis presented in this study represent an attempt to maximise the information that can be gleaned from the available records, recognizing that such records are not able to resolve (and therefore remove) such signals as the quasi-60-year ocean oscillation at the regional level, specific to South Korea. This issue might be addressed in future studies by considering the availability of much longer regional time series

capable of resolving such a signal and using the relevant portion of that signal as a proxy for application to the South Korean records.

Notwithstanding, the analysis techniques used identify the lowest-frequency signal (or trend) permitted by the length of the data sets available.

Estimating VLM

Land motions embedded within tide-gauge records are difficult contributions to resolve and isolate, in part because the general scale of VLMs (see Ostanciaux *et al.*, 2012) and sea-level rise trends due to climate change observed over the 20th and early 21st centuries are often of similar scale (although the sign may differ). In attempting to convert relative to geocentric estimates of sea-level rise, the majority of contemporary studies make some allowance for land movements via the application of site-specific estimates of long timescale Glacial Isostatic Adjustment (GIA) from the various models available (*e.g.,* Lambeck, Smither, and Johnston, 1998; Peltier, 2004; Tushingham and Peltier, 1991).

Watson (2016a) notes that GIA models provide only the broadest-scale resolution of VLMs at local scales. Local processes associated with tectonics, volcanism, sediment compaction, and subsurface mineral and water extraction are often of significance and generally not accounted for in the GIA models (Zervas, Gill, and Sweet, 2013). Tide gauges situated on highly urbanised and densely populated shorelines are becoming increasingly affected by a wide range of anthropogenic processes that predominantly result in localised subsidence (Ostanciaux *et al.*, 2012). The advent of the global navigation satellite system has provided the opportunity to continuously measure the total contributions of all land-movement processes where GPS recording instruments have been installed, enabling estimates of geocentric mean sea level (to a fixed reference point). The drawback of the comparatively recent development of these measuring technologies is that maximum record lengths are only around 20 years.

Another factor highlighted previously by Wöppelmann and Marcos (2012) relates to the common situation where the geodetic connection between the GPS antennae and tide gauge is absent. Under these circumstances it is simply assumed that vertical land movement sensed by the GPS antenna corresponds to the actual land movement affecting the tide-gauge record when the GPS antenna is distant from the tide gauge (*e.g.,* Bevis, Scherer, and Merrifield, 2002). This is a ubiquitous problem highlighted in the current study whereby only one active Système d'Observations du Niveau des Eaux Littorales (SONEL) (SONEL, 2018) GPS record exists within the study area (Incheon), and this recording instrument is located some 31.5 km from the tide gauge, diminishing the inferred representativeness of land-motion factors directly at the tide gauge.

SONEL provides VLM estimates at nine coastal sites around South Korea based on the inferred difference between satellite altimetry and the tide-gauge record over the period from 15 January 1993 to 15 November 2013 as part of an experimental endeavour. The current study provides updated estimates of VLM at a larger range of sites (21) over a longer period of time based on similar analytical procedures (Ostanciaux *et al.*,

2012). VLM determined via these processes are quite sensitive to the time frame of analysis, but such processes are envisaged to provide increasingly improved proxies for the actual rate of VLM at the tide gauge as the altimetry record lengthens.

In theory the difference between satellite altimetry and the tide-gauge record can reveal drifts in the altimeter or in its geophysical corrections, and also in the tide-gauge data. An important assumption is that these are negligible, so that the trend in the differences can be attributed to VLM (G. Wöppelmann, *personal communication*). It is important to appreciate that there will always be difficulties in directly assimilating data from such different measuring techniques. Although most modern tide-gauge records are highly accurate continuous data streams at a fixed location, the validity of sea-surface height measurements from satellite altimeters in coastal areas decreases significantly because of land contamination (Xu, Birol, and Cazenave, 2018), requiring substantial geophysical corrections (amongst others).

Capet *et al*. (2014) note that converting raw satellite sensor signals to accessible and exploitable gridded products (such as those used in the current study from AVISO) involves several processing steps, each of which is a compromise between the filtering out of observational noise and the retention of the most relevant part of the original signal (Ducet, Le Traon, and Reverdin, 2000; Le Traon and Dibarboure, 1999). Kleinherenbrink, Riva, and Frederikse (2018) advise that the larger effective radius of the AVISO products draws on data far away from the tide-gauge location, which might not correlate with the sea-level signal at the gauge, resulting in potential contamination of VLM trend estimates.

For sea-level studies, it is commonly assumed that VLMs are generally small and occur in near-linear fashion, in which case estimates of acceleration remain unaffected. Although geological timescale influences such as GIA will be approximately linear over the timescale of an available tide-gauge record, the anthropogenic influences contributing to subsidence in heavily developed coastal margins might not necessarily perpetuate in a linear manner (Watson, 2016a). The latter circumstance, if not properly accounted for, will contaminate real-time estimates of acceleration in the relative mean sea-level signal. Despite the above-mentioned range of issues associated with estimating VLM from the difference between satellite- and tide-gauge-derived products, such efforts provide a reasonable, convenient estimate around the coast in the absence of precise GPS-measured data.

Opportunities exist around South Korea to increase the density of GPS measuring devices colocated with tide gauges for improved scientific understanding of VLMs, mean sea level, and climate-change influences into the future.

Comparison with Previous Sea-Level Studies of South Korea

There has been a range of recent studies investigating mean sea-level trends and accelerations around South Korea using differing techniques and data (*e.g.*, Ha *et al*., 2006; Jeon, 2008; Kang *et al*., 2005; KHOA, 2013; Kim and Cho, 2016; Kim *et al*., 2017; Yoon, 2016). The majority of studies have involved linear regression analysis of available tide-gauge data. Kim *et al*. (2017) analysed eight mean sea-level records around the southeastern coast of Korea, using hourly data spanning ≈ 40 years (up to 2014). Simple linear regression analyses were applied to each of the data sets to estimate the average velocity (or trend) of relative mean sea level. The average trend across all data records was 2.75 mm/y. However, a key observation of the analysis was the high trend of 5.82 mm/y observed at Pohang, nearly 3 mm/y higher than any other site. Contributory reasons posed for such a high rate of rise included possible datum changes due to several harbour constructions or land subsidence. The current study confirms the high rate of VLM due to subsidence evident at Pohang (–7.4 mm/y).

Similarly, Yoon (2016) investigated the relative rise in mean sea level around the Korean Peninsula applying linear regression techniques to 19 station records with a minimum length of 30 years. Results suggested that rates of relative sea-level rise over the period of analysis were relatively small along the western coast (average 2.0 mm/y), large along the southern and eastern coasts (averages 2.8 and 3.6 mm/y, respectively), and very large around Jeju Island (average 3.8 mm/y).

Although linear regression is a simple and convenient application for determining a coarse, first-order trend, it is an ill-suited tool for the task at hand given the time-varying nature of the mean sea-level signal evident from contemporary analysis of the world's longest tide-gauge records (Watson, 2016a, 2017, 2018). Linear regression provides no temporal instruction on relevant changes in the mean sea-level velocity and acceleration time series, given the inherent assumptions of constant velocity and zero acceleration. Shorter time series such as those considered by Kim *et al*. (2017) and Yoon (2016), which are a maximum of 40 years in length, become increasingly influenced (or biased) by internal climate modes when simple linear regression is used to estimate the relative rate of mean sea-level rise.

Kim and Cho (2016) provide more advanced time-series analysis of the five longest records (Mokpo, Jeju, Busan, Ulsan, and Mukho) through the application of ensemble empirical mode decomposition (EEMD) (Wu and Huang, 2009) to define mean sea level and then central difference techniques to estimate the time-varying velocities and accelerations. This work appears to be the first attempt to consider acceleration in the Korean mean sea-level records.

Table 3 provides a summary of the minimum and maximum relative velocities at each station advised in the paper of Kim and Cho (2016) compared with those determined in the current study. Of interest, the maximum velocities determined via the study of Kim and Cho (2016) is ≈ 1 to 2 mm/y higher than those determined via the approaches advocated in the current study. However, the ordering of the station records on the basis of the maximum relative velocities between the respective approaches is equivalent. For example, the highest maximum relative velocity was observed at Mokpo and the lowest at Ulsan in both sets of analysis. The range between the minimum and maximum relative velocities at each station was also much higher for the approach of Kim and Cho (2016).

Kim and Cho (2016) advised that the highest acceleration from all stations was 0.143 ± 0.026 (1σ) mm/y^2 at Mokpo (year unknown), which is in agreement with the current study, which also advised a maximum acceleration of 0.14 ± 0.03 (1σ) mm/y^2 at Mokpo (in 2002).

Table 3. *Comparison of results of Kim and Cho (2016) with current study.*

| | Kim and Cho (2016)[†] | | Current study[‡] | |
Location	Min. velocity (mm/y)	Max. velocity (mm/y)	Min. velocity (mm/y)	Max. velocity (mm/y)
Mokpo	0.74	6.75	2.39 (1960)	5.83 (2015)
Jeju	3.78	6.34	5.09 (1964)	5.41 (2017)
Busan	−0.48	4.08	2.30 (1961)	2.75 (2017)
Ulsan	1.38	2.61	0.46 (1973)	0.90 (2016)
Mukho	−3.00	3.66	1.07 (1965)	2.14 (2017)

[†]*All velocities advised are relative rates of rise in mean sea level.*
[‡]*The year in which the respective maximum and minimum velocities occurred is indicated in parentheses. These details were not available from the paper of Kim and Cho (2016).*

Aspects of the results of the current study and those of Kim and Cho (2016) indicate similar nonlinear characteristics in the measured rates of relative velocity observed around South Korea. However, the higher velocities and ranges observed in the results of Kim and Cho (2016) are likely to be (at least in part) artefacts of the EEMD approach, likely retaining energy from higher-frequency signals due to mode mixing with the residual element, which is a feature exacerbated by the comparatively short data sets used (refer to Discussion).

Empirical mode decomposition (EMD) (Huang *et al.*, 1998) is known to have inherent limitations associated with mode mixing and splitting, aliasing, and end effects (Mandic *et al.*, 2013). The EEMD variant (Wu and Huang, 2009), which effectively combines EMD with noise stabilisation, was an enhancement designed to offset the propensity for mode mixing and aliasing (Tary *et al.*, 2014). EEMD, however, contains a further limitation in that the sum of the intrinsic mode functions determined by the algorithm doesn't necessarily reconstruct the original signal (Tary *et al.*, 2014).

Chambers (2015) evaluated the EMD algorithm for quantifying multidecadal variations and accelerations in sea-level records, concluding a range of issues with the approach and suggesting its use with considerable caution. Similarly, the most extensive time-series analysis testing for mean sea-level research undertaken to date (Watson, 2016b) concluded that data-adaptive spectral techniques such as SSA and multi-resolution decomposition using maximal overlap discrete wavelet transform (Percival and Walden, 2006) significantly outperformed all other time-series techniques (including EMD and EEMD) for isolating a trend with improved temporal resolution and accuracy from mean sea-level records.

CONCLUSION

The issue of sea-level rise is of particular interest around the Korean Peninsula given that the land mass is bounded to the east by the East Sea (Sea of Japan), to the south by the East China Sea, and to west by the Yellow Sea. Large coastal populations and extensive, built assets occupy the coastal regions of South Korea, with continued population growth and urban development forecast into the future.

In addition, the coastlines along the southeastern portions of the country are frequently affected by high storm-surge-generating typhoons, particularly during July to October (Kim *et al.*, 2017). The current threats associated with coastal

hazards (*e.g.*, coastal erosion, storm surge, oceanic inundation, *etc.*) will be exacerbated by projected sea-level rise associated with climate change that is anticipated to increase at an increasing rate over the course of the 21st century (and beyond).

With this in mind, every effort must be made to routinely monitor and review sea-level data around the country, enabling the early detection of key emerging trends of significance that will aid coastal planning, design, and risk-management activities. This study updates and extends the several previous works undertaken to analyse tide-gauge records and satellite altimetry around the Korean Peninsula using enhanced time-series analysis techniques to detect the current rates of rise and accelerations in mean sea level.

Analysis of the seven tide-gauge records exceeding 50 years in length indicates that the rate of relative mean sea-level rise (velocity) has continued to increase at each site through to 2017, suggesting acceleration to do so. The highest rates of relative mean sea-level rise were observed at Mokpo and Jeju (5.8 and 5.4 mm/y, respectively) over the recent portion of the record, driven in part by high rates of subsidence exceeding 3 mm/y. Mokpo in particular should be closely monitored, as this site has also experienced the highest rate of acceleration recorded at any site around the county.

General trends of subsidence were observed around the margins bounded by the East China Sea and East Sea (Sea of Japan) (below 36°N), whereas uplift was a more prevalent feature along the margins bounded by the Yellow Sea. Improved knowledge of VLMs is paramount as subsiding margins will exacerbate the threat posed by rising mean sea levels. Opportunities exist to colocate continuous-recording GPS technology with the seven long tide-gauge sites around the country to precisely measure critical land movements and augment the scientific value of these lengthening mean sea-level records.

In addition to the above-mentioned observations from key land-based records, the advent of routine satellite altimetry (post-1993) permits trend analysis of sea-surface heights at fixed closely spaced grid points across the ocean margins surrounding the country. This analysis highlights peak average sea-surface height trends centred in two discrete areas east and west of South Korea around 37.5°N that exceeded 8 mm/y over the past 24 years. It will be critical to continue to monitor these margins to ascertain whether or not these high trends become a more persistent regional oceanographic feature or whether they are governed by decaying or strengthening ENSO (or other internal climate mode) episodes.

When the satellite altimetry data are averaged over the respective margins of the Yellow Sea, East Sea (Sea of Japan), and East China Sea, the means differ and are all below the global average, with the South China Sea average ≈0.75 mm/y lower over the 24-year record. The trends in sea-surface heights are significantly influenced by internal climate mode forcings (such as ENSO, *etc.*) on such short timescales, but such trends should be carefully monitored along with the tide-gauge records to better understand the regional spatial characteristics of a rising mean sea level.

It is strongly recommended that the analysis presented in this report be revisited every 5 years or so to take advantage of ever-lengthening data records, improving time-series analysis

techniques, and scientific advancements concerning climate change and its influence on sea-level rise.

LITERATURE CITED

Alexandrov, T.; Bianconcini, S.; Dagum, E.B.; Maass, P., and McElroy, T.S., 2012. A review of some modern approaches to the problem of trend extraction. *Econometric Reviews*, 31(6), 593–624.

AVISO (Archiving, Validation and Interpretation of Satellite Oceanographic), 2018. http://www.aviso.altimetry.fr/duacs/.

Bevis, M.; Scherer, W., and Merrifield, M., 2002. Technical issues and recommendations related to the installation of continuous GPS stations at tide gauges. *Marine Geodesy*, 25(1–2), 87–99.

Calafat, F. and Chambers, D., 2013. Quantifying recent acceleration in sea level unrelated to internal climate variability. *Geophysical Research Letters*, 40(14), 3661–3666.

Capet, A.; Mason, E.; Rossi, V.; Troupin, C.; Faugère, Y.; Pujol, I., and Pascual, A., 2014. Implications of refined altimetry on estimates of mesoscale activity and eddy-driven offshore transport in the Eastern Boundary Upwelling Systems. *Geophysical Research Letters*, 41(21), 7602–7610.

Chambers, D.P., 2015. Evaluation of empirical mode decomposition for quantifying multidecadal variations and acceleration in sea level records. *Nonlinear Processes in Geophysics*, 22(2), 157–166.

Chambers, D.P.; Merrifield, M.A., and Nerem, R.S., 2012. Is there a 60-year oscillation in global mean sea level? *Geophysical Research Letters*, 39(18), doi: 10.1029/2012GL052885.

Church, J.A.; Clark, P.U.; Cazenave, A.; Gregory, J.M.; Jevrejeva, S.; Levermann, A.; Merrifield, M.A.; Milne, G.A.; Nerem, R.S.; Nunn, P.D.; Payne, A.J.; Pfeffer, W.T.; Stammer, D., and Unnikrishnan, A.S., 2013a. Sea level change. *In:* Stocker, T.F.; Qin, D.; Plattner, G-K.; Tignor, M.; Allen, S.K.; Boschung, J.; Nauels, A.; Xia, Y.; Bex, V., and Midgley, P.M. (eds.), *Climate Change 2013: The Physical Science Basis*. Contribution of Working Group I to the Fifth Assessment Report of the Intergovernmental Panel on Climate Change. Cambridge: Cambridge University Press, pp. 1137–1216.

Douglas, B.C., 2001. Sea level change in the era of the recording tide gauge. *International Geophysics*, 75, 37–64.

Ducet, N.; Le Traon, P.Y., and Reverdin, G., 2000. Global high-resolution mapping of ocean circulation from TOPEX/Poseidon and ERS-1 and-2. *Journal of Geophysical Research: Oceans*, 105(C8), 19477–19498.

Golyandina, N.; Nekrutkin, V., and Zhigljavsky, A.A., 2001. *Analysis of Time Series Structure: SSA and Related Techniques*. Boca Raton, Florida: Chapman and Hall/CRC, 320p.

Golyandina, N. and Zhigljavsky, A., 2013. *Singular Spectrum Analysis for Time Series*. Berlin: Springer Science & Business Media, 120p.

Ha, K.J.; Jeong, G.Y.; Jang, S.R., and Kim, K.Y., 2006. Variation of the sea surface height around the Korean peninsula with the use of multi-satellite data (Topex/Poseidon, Jason-1, ERS, Envisat) and its association with sea surface temperature. *Korean Journal of Remote Sensing*, 22(6), 519–531.

Hallegatte, S.; Green, C.; Nicholls, R.J., and Corfee-Morlot, J., 2013. Future flood losses in major coastal cities. *Nature Climate Change*, 3(9), 802–806.

Holgate, S.J.; Matthews, A.; Woodworth, P.L.; Rickards, L.J.; Tamisiea, M.E.; Bradshaw, E.; Foden, P.R.; Gordon, K.M.; Jevrejeva, S., and Pugh, J., 2012. New data systems and products at the permanent service for mean sea level. *Journal of Coastal Research*, 29(3) 493–504.

Houston, J.R. and Dean, R.G., 2013. Effects of sea-level decadal variability on acceleration and trend difference. *Journal of Coastal Research*, 29(5), 1062–1072.

Huang, N.E.; Shen, Z.; Long, S.R.; Wu, M.C.; Shih, E.H.; Zheng, Q.; Tung, C.C., and Liu, H.H., 1998. The empirical mode decomposition and the Hilbert spectrum for nonlinear and non-stationary time series analysis. *Proceedings of the Royal Society of London*. Series A: Mathematical, Physical and Engineering Sciences, 454(1971), 903–995.

ICDC (Integrated Climate Data Center), 2018. *AVISO SSH Data*. http://icdc.cen.uni-hamburg.de/1/daten/ocean/ssh-aviso.html.

Jeon, D.C., 2008. Relative sea-level change around the Korean Peninsula. *Ocean and Polar Research*, 30(4), 373–378.

Kahle, D. and Wickham, H., 2013. ggmap: Spatial visualization with ggplot2. *R Journal*, 5(1), 144–161.

Kang, S.K.; Cherniawsky, J.Y.; Foreman, M.G.G.; Min, H.S.; Kim, C.H., and Kang, H.W., 2005. Patterns of recent sea level rise in the East/Japan Sea from satellite altimetry and in situ data. *Journal of Geophysical Research: Oceans*, 110(C7).

KHOA (Korea Hydrographic and Oceanographic Agency), 2013. *Analysis and Prediction of Sea Level Change*. Busan, Republic of Korea: KHOA, 252p (in Korean).

Kim, D.Y.; Park, S.H.; Woo, S.B.; Jeong, K.Y., and Lee, E.I., 2017. Sea-level rise and storm surge around the southeastern coast of Korea. *In:* Lee, J.L.; Griffiths, T.; Lotan, A.; Suh, K.-S., and Lee, J. (eds.), 2nd International Water Safety Symposium. *Journal of Coastal Research*, Special Issue No. 79, pp. 239–243.

Kim, Y. and Cho, K., 2016. Sea level rise around Korea: Analysis of tide gauge station data with the ensemble empirical mode decomposition method. *Journal of Hydro-environment Research*, 11, 138–145.

Kleinherenbrink, M.; Riva, R., and Frederikse, T., 2018. A comparison of methods to estimate vertical land motion trends from GNSS and altimetry at tide gauge stations. *Ocean Science*, 14(2).

Kondrashov, D. and Ghil, M., 2006. Spatio-temporal filling of missing points in geophysical data sets. *Nonlinear Processes in Geophysics*, 13(2), 151–159.

Lambeck, K.; Smither, C., and Johnston, P., 1998. Sea-level change, glacial rebound and mantle viscosity for northern Europe. *Geophysical Journal International*, 134(1), 102–144.

Le Traon, P.L. and Dibarboure, G., 1999. Mesoscale mapping capabilities of multiple-satellite altimeter missions. *Journal of Atmospheric and Oceanic Technology*, 16(9), 1208–1223.

Mandic, D.P.; ur Rehman, N.; Wu, Z., and Huang, N.E., 2013. Empirical mode decomposition-based time-frequency analysis of multivariate signals: The power of adaptive data analysis. *IEEE Signal Processing Magazine*, 30(6), 74–86.

McGranahan, G.; Balk, D., and Anderson, B., 2007. The rising tide: Assessing the risks of climate change and human settlements in low elevation coastal zones. *Environment and Urbanization*, 19(1), 17–37.

Neumann, B.; Vafeidis, A.T.; Zimmermann, J., and Nicholls, R.J., 2015. Future coastal population growth and exposure to sea-level rise and coastal flooding—A global assessment. *PloS one*, 10(3), 0118571, https://doi.org/10.1371/journal.pone.0118571.

Ostanciaux, É.; Husson, L.; Choblet, G.; Robin, C., and Pedoja, K., 2012. Present-day trends of vertical ground motion along the coast lines. *Earth-Science Reviews*, 110(1), 74–92.

Peltier, W.R., 2004. Global glacial isostasy and the surface of the ice-age earth: The ICE-5G(VM2) model and GRACE. *Annual Review of Earth and Planetary Sciences*, 32, 111–149.

Percival, D.B. and Walden, A.T., 2006. *Wavelet Methods for Time Series Analysis, Volume 4*. Cambridge: Cambridge University Press, 622p.

PSMSL (Permanent Service for Mean Sea Level), 2018. http://www.psmsl.org.

Qiu, B. and Chen, S., 2012. Multidecadal sea level and gyre circulation variability in the northwestern tropical Pacific Ocean. *Journal of Physical Oceanography*, 42(1), 193–206.

R Core Team, 2018. R: A language and environment for statistical computing. R Foundation for Statistical Computing, Vienna, Austria. ISBN 3-900051-07-0. http://www.R-project.org/.

SONEL (Système d'Observation du Niveau des Eaux Littorales), 2018. http://www.sonel.org/-Vertical-land-movement-estimate-.html.

Sturges, W. and Douglas, B.C., 2011. Wind effects on estimates of sea level rise. *Journal of Geophysical Research: Oceans*, 116(C6), doi: 10.1029/2010JC006492.

Tary, J.B.; Herrera, R.H.; Han, J., and Baan, M., 2014. Spectral estimation—What is new? What is next? *Reviews of Geophysics*, 52(4), 723–749.

Tushingham, A. and Peltier, W.R., 1991. Ice-3G: A new global model of late Pleistocene deglaciation based upon geophysical predictions of post-glacial relative sea level change. *Journal of Geophysical Research: Solid Earth*, 96(B3), 4497–4523.

Watson, P.J., 2016a. Acceleration in U.S. mean sea level? A new insight using improved tools. *Journal of Coastal Research*, 32(6), 1247–1261.

Watson, P.J., 2016b. Identifying the best performing time series analytics for sea-level research. *In:* Rojas, I. and Pomares, H. (eds.), *Time Series Analysis and Forecasting: Contributions to Statistics*. Basel, Switzerland: Springer, pp. 261–278, doi:10.1007/978-3-319-28725-6.

Watson, P.J., 2017. Acceleration in European mean sea level? A new insight using improved tools. *Journal of Coastal Research*, 33(1), 23–38.

Watson, P.J., 2018. Improved Techniques to Estimate Mean Sea Level, Velocity and Acceleration from Long Ocean Water Level Time Series to Augment Sea Level (and Climate Change) Research. Sydney, Australia: University of New South Wales, Ph.D dissertation, 199p.

Wöppelmann, G. and Marcos, M., 2012. Coastal sea level rise in southern Europe and the non-climate contribution of vertical land motion. *Journal of Geophysical Research: Oceans*, 117(C1), doi: 10.1029/2011JC007469.

Wu, Z. and Huang, N.E., 2009. Ensemble empirical mode decomposition: A noise-assisted data analysis method. *Advances in Adaptive Data Analysis*, 1(01), 1–41.

Xu, X.Y.; Birol, F., and Cazenave, A., 2018. Evaluation of coastal sea level offshore Hong Kong from Jason-2 altimetry. *Remote Sensing*, 10(2), 282.

Yeora, C., 2012. *The Economic Analysis of Climate Change in South Korea*. Report published by Korea Adaptation Center for Climate Change (KACCC).

Yoon, J.J., 2016. Analysis of long-period sea-level variation around the Korean Peninsula. *In:* Vila-Concejo, A.; Bruce, E.; Kennedy, D.M., and McCarroll, R.J. (eds.), *Proceedings of the 14th International Coastal Symposium (ICS) 2016* (Sydney, Australia). *Journal of Coastal Research,* Special Issue, No. 75, pp. 1432–1436.

Zervas, C.; Gill, S., and Sweet, W., 2013. *Estimating Vertical Land Motion from Long-Term Tide Gauge Records*. NOAA Technical Report. NOS CO-OPS, 65, p. 22.